Steel and Composite Structures, *Vol. 30, No. 1 (2019) 31-46*
DOI: https://doi.org/10.12989/scs.2019.30.1.031

Dynamic characterization of a CNT reinforced hybrid uniform and non-uniform composite plates

Jakkamputi Lakshmipathi [1] and Rajamohan Vasudevan [*2]

[1] *School of Mechanical and Building sciences Engineering, Vellore Institute of Technology (VIT), Chennai 600127, Tamil Nadu, India*
[2] *School of Mechanical Engineering, Vellore Institute of Technology (VIT), Vellore 632014, Tamil Nadu, India*

(*Received May 3, 2018, Revised December 22, 2018, Accepted December 31, 2018*)

Abstract. In the present study, the various dynamic properties of MWCNT embedded fiber reinforced polymer uniform and tapered composite (MWCNT-FRP) plates are investigated. Various configurations of a tapered composite plate with ply-drop off and uniform composite plate have been considered for the development of the finite element formulation and experimental investigations. First order shear deformation theory (FSDT) has been used to derive the kinetic and potential energy equations of the hybrid composite plates by including the effect of rotary inertia, shear deformation and non-uniformity in thickness of the plate. The governing equations of motion of FRP composite plates without and with MWCNT reinforcement are derived by considering a nine- node rectangular element with five degrees of freedom (DOF) at each node. The effectiveness of the developed finite element formulation has been demonstrated by comparing the natural frequencies and damping ratio of FRP composite plates without and with MWCNT reinforcement obtained experimentally. Various parametric studies are also performed to study the effect of CNT volume fraction and CNT aspect ratio of the composite plate on the natural frequencies of different configurations of CNT reinforced hybrid composite plates. Further the forced vibration analysis is performed to compare the dynamic response of the various configurations of MWCNT-GFRP composite plate with GFRP composite plate under harmonic excitations. It was observed that the fundamental natural frequency and damping ratio of the GFRP composite plate increase approximately 8% and 37% respectively with 0.5wt% reinforcement of MWCNT under CFCF boundary condition. The natural frequencies of MWCNT-GFRP hybrid composite plates tend to decrease with the increase of MWCNT volume fraction beyond 2% due to agglomeration of CNT's. It is also observed that the aspect ratio of the CNT has negligible effect on the improvement of dynamics properties due to randomly orientation of CNT's.

Keywords: CNT reinforced composite plates; Modal analysis; vibration; dynamic characterization

1. Introduction

Fiber reinforced composites (FRP) are engineered materials which have gained significant importance in the high performance structural applications such as aerospace, automotive, marine and infrastructure. Composite materials used in such applications require high strength, stiffness and vibration damping ability. However, these structural materials suffer low damping characteristics which result in reduced performance and life cycle, structural damage, annoying noise and discomfort. The damping ability of the structures is improved by active, semi-active and passive vibration control techniques. Even though active system provides fast vibration suppression of the structures, the applications are narrowed due to expensive in implementation, external power consumption, weight and routine maintenance. On the other hand, the semi active vibration control system (magneto rheological materials) provide better damping capability at the expense of the increase in mass of the structures. Multi walled carbon nanotubes (MWCNTs) are attractive for use as secondary fillers in composite materials that contain continuous fibers as primary fillers. In contrast to MR materials, MWCNTs intensify the damping ability due to slippage between MWCNTs and the matrix in the large interface area per unit volume along with enhanced mechanical properties of the composite (Thostenson *et al*. 2001, Lau 2003 and Zhou *et al*. 2004) without any significant change in mass of the structure. Before these remarkable properties of MWCNTs combined with low density are realized in macroscopic composite, knowledge of characterization techniques and micro-models to estimate the elastic behavior of MWCNTs and interface of nanotubes and matrix are necessary.

The challenges in the dispersion of carbon nanotubes (CNTs) into matrix are quite different from the microscale fibers such as Al_2O_3 and carbon particles. Moreover, pristine MWCNTs are highly entangled bundles of few hundreds of individual CNTs (Gong *et al*. 2000). The mechanical properties of CNT composites are attenuated due to the agglomerated and entangled nanotubes. Researchers proposed different dispersion techniques such as functionalization and physical blending to overcome the challenges in composite material processing (Gong *et al*. 2000). In functionalization process, the surface of CNT is modified to disintegrate the CNT bundles into individuals and disperse uniformly into the low viscous polymers.

*Corresponding author, Professor,
E-mail: vasudevan.r@vit.ac.in

http://www.techno-press.org/?journal=scs&subpage=6
ISSN: 1229-9367 (Print), 1598-6233 (Online)

Several models were developed to predict the elastic, static and dynamic behavior of the CNT composite plates. The micromechanical models such as Halpin–Tsai equation (Qian *et al*. 2000, Yeh *et al*. 2009, Montazeri *et al*. 2010), extended rule of mixture (Omidi *et al*. 2010) and Eshelby–Mori–Tanaka approach (Lei *et al*. 2013) were developed in the literature to study the elastic behavior of isotropic matrix in CNT reinforced composites. These models are proposed to include the correction factors for orientation of CNT, nonlinear behavior of CNT and randomness of discontinuous fibers. Out of all the models, the modified Halpin–Tsai model is rather sophisticated to predict the mechanical properties of CNT embedded polymer matrix.

The MWCNT based polymer composite can improve both the natural frequencies and damping capabilities of structural applications. Thostenson and Chou (2003) reported improvement in average elastic modulus of Polystyrene by 42% and 84% with 5 wt% and 10 wt % of CNT content, respectively. Bai and Allaoui (2003) experimentally found decrease in efficiency rate of Young's modulus of nanocomposite with increasing CNT content. Ashrafi and Hubert (2006) numerically found insignificant effect of nanotube length on the elastic properties of SWNT polymer composites. According to Montazeri and Montazeri (2011), the modulus of polymer composite is increased by 23% with addition of 2 wt% of MWCNT. A 500% increase in fundamental natural frequency of rubber was reported in Formica *et al*. (2010) by adding 1% volume fraction of CNT. Zhu *et al*. (2012) numerically reduce the central deflection of CNTRC plates by 30% with 6% increase in the volume fraction of CNT. Jakkamputi and Rajamohan (2017) studied the effect of temperature on the elastic modulus and dynamic properties of hybrid composite beam made up of CNT reinforcement in polymer matrix. It was demonstrated that the fundamental natural frequency could be increased by 19% with the addition of 0.5 wt% CNT to glass fiber reinforced polymer composite beam. Wang *et al*. (2018) numerically found 47% improvement in the non-dimensional fundamental frequency of sandwich plate with CNT reinforced face sheets with the increase of CNT volume fraction from 0.12 to 0.28. Rafiee *et al*. (2018) experimentally improved the fundamental natural frequency of CNT nanocomposite by approximately 9% with the addition of 0.02 wt% of functionalized MWCNT.

Rajoria and Jalili (2005) demonstrated that damping of epoxy composite is increased by 700% by using 5 wt% of CNT. Yeh and Hsieh (2008) reported that 40% improvement in the loss factor of sandwich beams with CNT-epoxy core could be achieved by incorporating 2wt% of CNT in polymer. The damping of CNT nano composites was found to be dependent on strain and increases up to 350% compared with pure epoxy resins (Lau 2003, Dai and Liao 2009). Khan *et al*. (2011) improved damping ratio of CFRP composite plate by 50% with addition of 1wt% of MWCNT. DeValve and Pitchumani (2011) showed that the damping could be increased by 130% and 150%, respectively in stationary beam and in rotating composite beam by embedding 2 wt% of CNT into carbon fiber

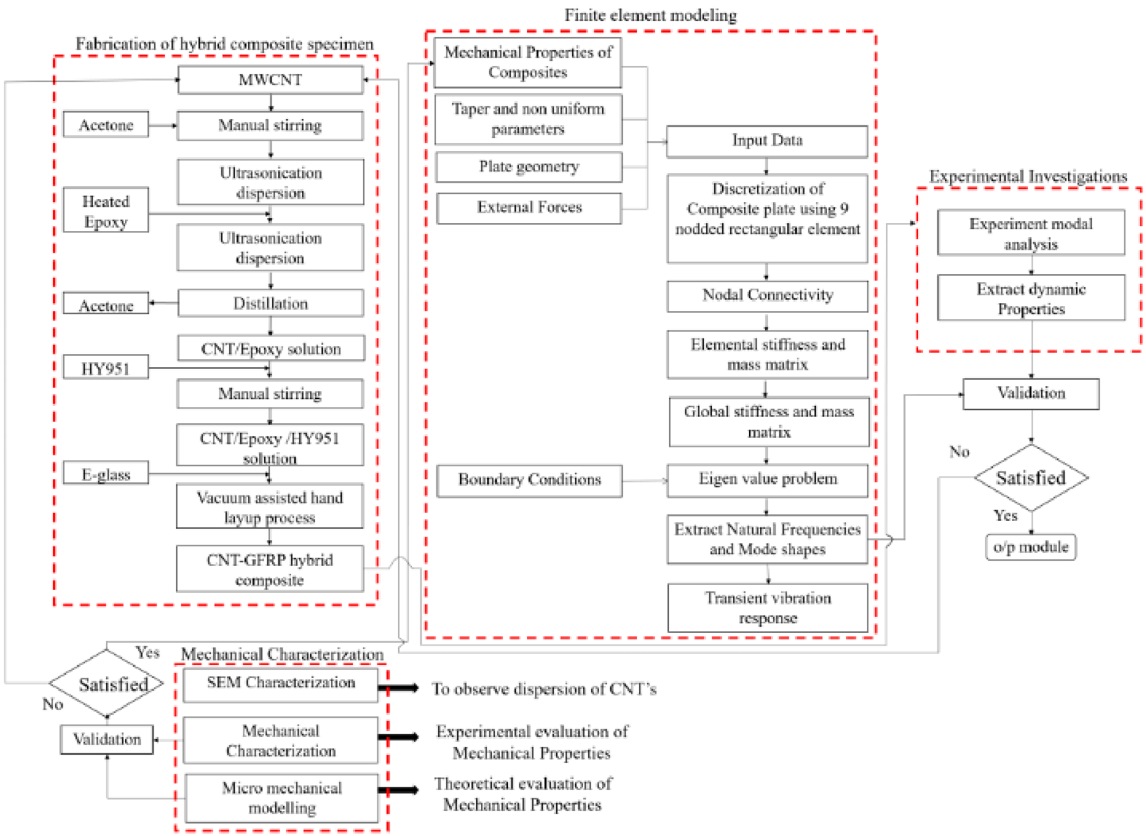

Fig. 1 Various steps involved in fabrication, experimental analysis and numerical simulation of MWCNT-FRP composite plate

reinforced polymer composite.

Although much research in the literature has evident for the dynamic characterization of CNT reinforced polymer nanocomposites, there has been limited numerical simulation and experimental studies on dynamic characterization of CNT embedded continuous fiber reinforced polymer composite plates (CNT-FRP). These hybrid nanocomposites are necessary to achieve high stiffness and damping for high performance structural applications.

The present work investigates the dynamic properties of MWCNT embedded fiber reinforced polymer tapered composite (CNTCNT-FRP) plates. Various configurations of a tapered composite plate with ply-drop off have been considered for the development of the finite element formulation and experimental investigations. First order shear deformation theory (FSDT) has been used to derive the kinetic and potential energy equations of the uniform and various configurations of tapered composite plates by including the effect of rotary inertia, shear deformation and non-uniformity in thickness of the plate. The governing equations of motion of FRP composite plates without and with MWCNT reinforcement are derived by considering a nine-node rectangular elements with five degrees of freedom (DOF) at each node. The effectiveness of the finite element formulation has been demonstrated by comparing the natural frequencies and damping ratios of FRP tapered composite plates without and with CNT reinforcement obtained experimentally. Fig. 1 shows the various steps followed in fabrication, experimental analysis and numerical simulation of CNT reinforced hybrid composite plate.

Various parametric studies are also performed to study the effect of MWCNT volume fraction, MWCNT aspect ratio, and aspect of the composite plate on the natural frequencies of different tapered configurations of MWCNT reinforced hybrid composite plates. Further, the forced vibration analysis is performed to study the dynamic response of the various MWCNT-FRP taper composite plates under harmonic excitations.

2. Mathematical modeling of the CNT reinforced hybrid uniform and tapered composite plates

A uniform and various configurations of a tapered CNT reinforced hybrid polymer composite plates with length (L) and width (B) and height (H) are considered as shown in Fig. 2 for the development of governing equation of transverse vibration response. The uniform composite plate has been represented as "C0 configuration" (Fig. 2(a)) while the tapered composite plates are represented as "C1", "C2" and "C3" (Figs. 2(b)-(d)) whose thickness varies linearly along the axial direction x. All the tapered configurations are divided into four regions along axial direction with one ply above and below the mid plane surface dropped off in each region to form a tapered configuration. C1 and C3 configurations are customized with oblique, horizontal plies and resin pockets along axial direction x by dropping continuous horizontal and alternate horizontal plies in each region (Figs. 2(b) and (d)) whereas the tapered configuration C2 is customized with oblique and resin pockets along axial direction x by dropping continuous oblique plies (Fig. 2(c)). The thickness of the tapered configurations is assumed to be H_L at the left end and H_R at the right end of the composite plate. The MWCNT reinforcement of all the configurations is assumed to be distributed uniformly with identical volume fraction.

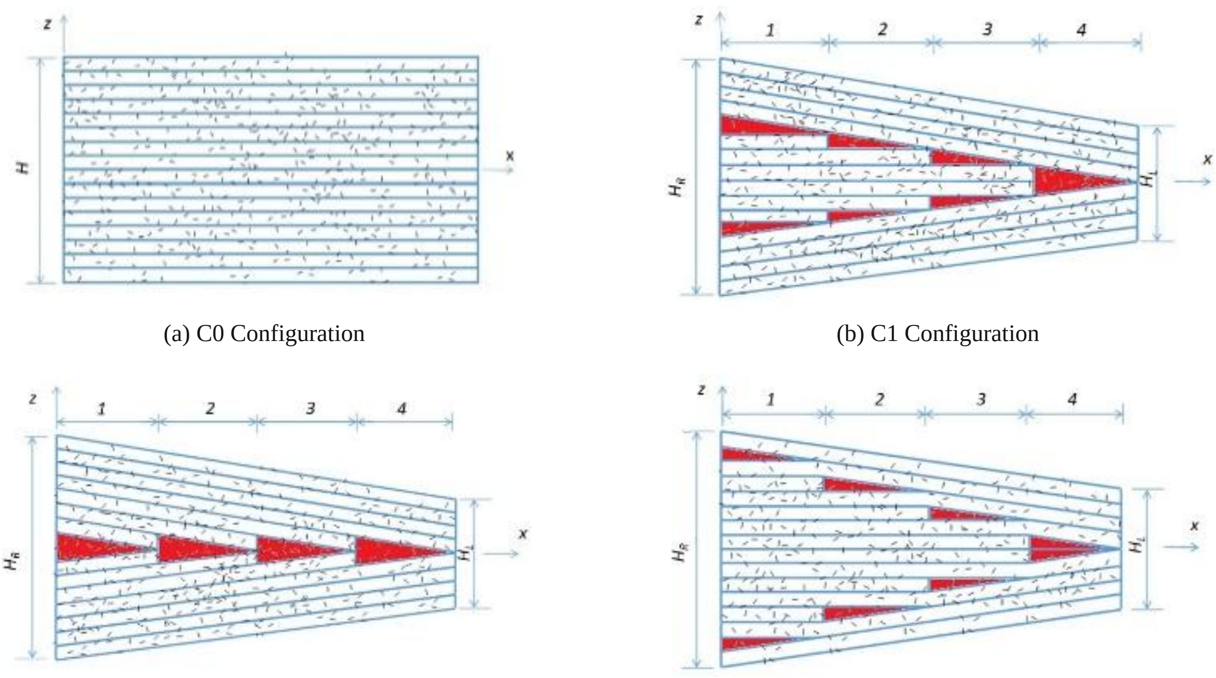

(a) C0 Configuration

(b) C1 Configuration

(c) C2 Configuration

(d) C3 Configuration

Fig. 2 Representation of various tapered configurations

2.1 Micro-mechanical modeling of CNTs reinforced polymer composite

In this work, the effective mechanical properties of the CNT polymer matrix are obtained based on modified Halpin-Tsai model proposed by Yeh *et al*. (2009) and Montazeri *et al*. (2010). These models are further modified to include the effect of random orientation of CNT in the matrix (Mallick 2007) such that:

Young's modulus of CNT/epoxy matrix (E_m) is expressed as

$$E_m = \left(\frac{3}{8}\right)E_{pl} + \left(\frac{5}{8}\right)E_{pt} \tag{1}$$

Shear modulus of CNT/epoxy matrix (G_m) is expressed as (Mallick 2007)

$$G_m = \left(\frac{1}{8}\right)E_{pl} + \left(\frac{1}{4}\right)E_{pt} \tag{2}$$

Where

$$E_{p_l} = \frac{1+2\zeta\eta_L v_{CNT}}{1-\eta_L v_{CNT}}E_p\ , \quad E_{p_t} = \frac{1+2\eta_T v_{CNT}}{1-\eta_T v_{CNT}}E_p \tag{3}$$

Density of CNT/epoxy matrix (ρ_m) is expressed as

$$\rho_m = v_{CNT}\rho_{CNT} + v_P\rho_P \tag{4}$$

E_m, G_m, υ_m, ρ_m and v_{CNT} are Young's modulus, rigidity modulus, Poisson ratio, density of isotropic matrix (CNT-epoxy) and volume fraction of CNT respectively. E_{Pl} and E_{pt} are longitudinal and transverse modulus of the unidirectional CNT epoxy lamina and η_L and η_T are the non-dimensional parameters which are calculated using Eqs. (1)-(3) by substituting the experimentally measured Young's moduli E_{Pl} and E_{pt}. ζ is exponential shape factor (Montazeri *et al*. 2010).

2.2 Macro-mechanical modeling of CNTs mixed hybrid fiber reinforced composite

The mechanical properties of the uniform and non-uniform configurations of CNT reinforced hybrid composite lamina are obtained based on rule of mixture.

Young's modulus of composite in longitudinal direction (E_{11}) is expressed as

$$E_{11} = v_f E_f + (1-v_f)E_m \tag{5}$$

Young's modulus of composite in transverse direction (E_{22}) is expressed as (Hashin 1970)

$$E_{22} = \frac{4KG_{23}}{K+mG_{23}} \tag{6}$$

In-plane shear modulus (1-2 plane) of composite (G_{12}) is expressed as

$$G_{12} = G_m\left[\frac{(1-v_f)+\gamma(1+v_f)}{(1+v_f)+\gamma(1-v_f)}\right] \tag{7}$$

Transverse shear modulus (2-3 plane) of composite (G_{23}) is expressed as

$$G_{23} = G_m\left[\frac{(1+\alpha v_f{}^2)(\mu+\beta_m v_f)-3v_f(1-v_f)^2\beta_m{}^2}{(1+\alpha v_f{}^2)(\mu-\beta_f)-3v_f(1-v_f)^2\beta_m{}^2}\right] \tag{8}$$

Major Poisson's ratio (1-2 Plane) of composite (υ_{12}) is expressed as

$$\upsilon_{12} = v_f\upsilon_f + (1-v_f)\upsilon_m \tag{9}$$

Density of composite (ρ_c) is expressed as

$$\rho_c = v_f\rho_f + (1-v_m)\rho_m \tag{10}$$

Where

$$\alpha = \frac{\beta_m-\gamma\beta_f}{1+\beta_f},\quad \mu = \frac{\gamma+\beta_m}{\gamma-1},\ \beta_m = \frac{1}{3-4\upsilon_m}$$
$$\beta_f = \frac{1}{3-4\upsilon_f},\ m = 1+4K\frac{\upsilon_{12}^2}{E_{11}} \tag{11}$$
$$K = \frac{K_m(K_f+G_m)v_m + K_f(K_m+G_m)v_f}{(K_f+G_m)v_m+(K_m+G_m)v_f}$$

The non-dimensional parameter γ is evaluated by substituting the experimentally measured in-plane shear modulus (G_{12}) of CNT reinforced hybrid polymer composite and Eq. (7). E_f, v_f and υ_f are Young's modulus, volume fraction and Poisson ratio of glass fiber.

2.3 Structural modelling of CNT reinforced hybrid composite plates

2.3.1 Strain and kinetic energy formulation

The first order shear deformation theory (FSDT) has been considered to develop the strain and kinetic energy relations by including the effects of rotory inertia and shear deformation of the various configurations of composite plates. The displacement field consisting of the axial deformation *u* and *v* along *x*-axis and *y*-axis, respectively and transverse displacement *w* along *z*-axis can be written as

$$\begin{aligned} u(x,y,z,t) &= u_0(x,y,t) + z\psi_y(x,y,t) \\ v(x,y,z,t) &= v_0(x,y,t) + z\psi_x(x,y,t) \\ w(x,y,z,t) &= w_0(x,y,t) \end{aligned} \tag{12}$$

Where u_0, v_0 and w_0 are the midplane displacements of the hybrid composite plate along *x*, *y* and *z* directions. Ψ_x and Ψ_y are the bending rotations of the cross section at any point with respect to *y* and *x* directions of the plate, respectively and *t* is time. FSDT assumes transverse normals of the plate before deformation remains straight but no longer normal in the deformed configurations which results in rotation of transverse normals. These assumptions cause constant transverse shear strain and stresses along the thickness of the beam. The shear correction factor (κ), equals to 5/6, was assumed to correct the difference between the constant shear strains and stresses in the FSDT and the actual distribution of shear strains and stresses.

The linear strain field is given by

$$\begin{Bmatrix} \varepsilon_{xx} \\ \varepsilon_{yy} \\ \gamma_{xy} \end{Bmatrix} = \varepsilon_0 + zk, \begin{Bmatrix} \gamma_{yz} \\ \gamma_{zx} \end{Bmatrix} = \gamma_0 \tag{13}$$

Where

$$\varepsilon_0 = \begin{Bmatrix} \frac{\partial u_0}{\partial x} \\ \frac{\partial v_0}{\partial y} \\ \frac{\partial u_0}{\partial y} + \frac{\partial v_0}{\partial x} \end{Bmatrix}, \quad \mathrm{k} = z\begin{Bmatrix} \frac{\partial \psi_x}{\partial x} \\ \frac{\partial \psi_y}{\partial y} \\ \frac{\partial \psi_x}{\partial y} + \frac{\partial \psi_y}{\partial x} \end{Bmatrix}, \quad \gamma_0 = \begin{Bmatrix} \psi_x + \frac{\partial w_0}{\partial y} \\ \psi_y + \frac{\partial w_0}{\partial x} \end{Bmatrix} \tag{14}$$

Then the linear stress ($\bar{\sigma}$) – strain ($\bar{\varepsilon}$) relationship of the composite plate along 1, 2 and 3 directions is expressed as

$$\overline{\sigma} = \overline{Q}\,\overline{\varepsilon} \tag{15}$$

Where

$$\overline{\sigma} = \begin{Bmatrix} \sigma_{11} \\ \sigma_{22} \\ \tau_{12} \\ \tau_{23} \\ \tau_{31} \end{Bmatrix}, \overline{Q} = \begin{bmatrix} Q_{11} & Q_{12} & 0 & 0 & 0 \\ Q_{21} & Q_{22} & 0 & 0 & 0 \\ 0 & 0 & Q_{66} & 0 & 0 \\ 0 & 0 & 0 & Q_{44} & 0 \\ 0 & 0 & 0 & 0 & Q_{55} \end{bmatrix}, \overline{\varepsilon} = \begin{Bmatrix} \varepsilon_{11} \\ \varepsilon_{22} \\ \gamma_{12} \\ \gamma_{23} \\ \gamma_{31} \end{Bmatrix} \tag{15}$$

$$\begin{gathered} Q_{11} = \left(\frac{E_{11}}{1-\upsilon_{12}\upsilon_{21}}\right), Q_{22} = \left(\frac{E_{22}}{1-\upsilon_{12}\upsilon_{21}}\right), \\ Q_{12} = \left(\frac{\upsilon_{21}E_{11}}{1-\upsilon_{12}\upsilon_{21}}\right),\ Q_{66} = G_{12}, Q_{44} = G_{23}\ and\ Q_{55} = G_{31} \end{gathered} \tag{16}$$

The linear constitutive stress (σ) – strain (ε) relations of the orthotropic lamina of the CNT reinforced hybrid polymer composite with respective to global coordinates are expressed as

$$\sigma = Q\,\varepsilon \tag{17}$$

Where

$$\begin{gathered} Q = [T\sigma\alpha][T\sigma\theta]\left[\overline{Q}\right][T\sigma\theta]^T[T\sigma\alpha]^T \\ \sigma = \begin{Bmatrix} \sigma_{xx} \\ \sigma_{yy} \\ \tau_{xy} \\ \tau_{yz} \\ \tau_{zx} \end{Bmatrix}, \ \{\varepsilon\} = \begin{Bmatrix} \varepsilon_{xx} \\ \varepsilon_{yy} \\ \gamma_{xy} \\ \gamma_{yz} \\ \gamma_{zx} \end{Bmatrix} \end{gathered} \tag{18}$$

$T_{\sigma\theta}$ is the transformation matrix from principal material coordinates (1, 2, 3) to the (X, Y, Z) coordinate system. The oblique plies of the different tapered configurations below the mid-plane have a positive oblique angle, α and the other oblique plies above the mid-plane have negative oblique angle, α. The horizantal plies above and below the mid plane have zero oblique angle. The transformation matrix ($T_{\sigma\alpha}$) is used to express the linear constitutive relations of the orthotropic lamina of the CNT reinforced hybrid polymer composite with respective to (x, y, z).

The strain energy (U) expression of CNT reinforced hybrid composite is expressed as

$$U = \frac{1}{2}\int \{\hat{u}\}^T \left[\hat{K}\right]\{\hat{u}\}\,dA \tag{19}$$

Where

$$\begin{gathered} \left[\hat{K}\right] = \begin{bmatrix} \frac{\partial}{\partial x} & 0 & 0 & 0 & 0 \\ 0 & \frac{\partial}{\partial y} & 0 & 0 & 0 \\ \frac{\partial}{\partial y} & \frac{\partial}{\partial x} & 0 & 0 & 0 \\ 0 & 0 & 0 & \frac{\partial}{\partial x} & 0 \\ 0 & 0 & 0 & 0 & \frac{\partial}{\partial y} \\ 0 & 0 & 0 & \frac{\partial}{\partial y} & \frac{\partial}{\partial x} \\ 0 & 0 & \frac{\partial}{\partial y} & 0 & 1 \\ 0 & 0 & \frac{\partial}{\partial x} & 1 & 0 \end{bmatrix}^{\mathrm{T}} \begin{bmatrix} A & B & 0 \\ B & D & 0 \\ 0 & 0 & A^s \end{bmatrix} \begin{bmatrix} \frac{\partial}{\partial x} & 0 & 0 & 0 & 0 \\ 0 & \frac{\partial}{\partial y} & 0 & 0 & 0 \\ \frac{\partial}{\partial y} & \frac{\partial}{\partial x} & 0 & 0 & 0 \\ 0 & 0 & 0 & \frac{\partial}{\partial x} & 0 \\ 0 & 0 & 0 & 0 & \frac{\partial}{\partial y} \\ 0 & 0 & 0 & \frac{\partial}{\partial y} & \frac{\partial}{\partial x} \\ 0 & 0 & \frac{\partial}{\partial y} & 0 & 1 \\ 0 & 0 & \frac{\partial}{\partial x} & 1 & 0 \end{bmatrix} \\ \{\hat{u}\} = \{\hat{u}_0\ \ \hat{v}_0\ \ \hat{w}_0\ \ \hat{\psi}_x\ \ \hat{\psi}_y\}^T \end{gathered} \tag{20}$$

in which the extensional A_{ij}, coupling B_{ij}, bending D_{ij}, and transverse shear A^s_{ij} stiffness are given by

$$\left(A_{ij}, B_{ij}, D_{ij}\right) = \sum_{1}^{n} \int_{h_k}^{h_{k-1}} Q_{ij}(1, z, z^2)dz; \quad i, j = 1,2,6$$
$$A_{ij}^{s} = \kappa \sum_{1}^{n} \int_{h_k}^{h_{k-1}} Q_{ij}dz; \quad i, j = 4, 5 \tag{21}$$

where

$$h_k = z_p + x \tan\alpha, h_{k-1} = z_{p-1} + x \tan\alpha \tag{22}$$

z_p and z_{p-1} are z coordinates of the top and bottom layers of the p^{th} lamina of the hybrid composite plate and α is the oblique angle of the tapered plies and zero for the horizantal plies and n is number of plies in each configuration and κ is the shear correction factor.

The kinetic energy expression (T) of CNT reinforced hybrid composite is given by

$$T = \frac{1}{2}\int \left\{\dot{\hat{u}}\right\}^T \left[\hat{M}\right]\left\{\dot{\hat{u}}\right\}dA \tag{23}$$

Where

$$\left[\hat{M}\right] = \begin{bmatrix} I_0 & 0 & 0 & I_1 & 0 \\ 0 & I_0 & 0 & 0 & I_1 \\ 0 & 0 & I_0 & 0 & 0 \\ I_1 & 0 & 0 & 2I_2 & 0 \\ 0 & I_1 & 0 & 0 & 2I_2 \end{bmatrix}, \left\{\dot{\hat{u}}\right\} = \begin{Bmatrix} \dot{\hat{u}}_0 \\ \dot{\hat{v}}_0 \\ \dot{\hat{w}}_0 \\ \dot{\hat{\psi}}_x \\ \dot{\hat{\psi}}_y \end{Bmatrix} \tag{24}$$
$$\left(I_0, I_1, I_2\right) = \sum_{1}^{n} \int_{h_k}^{h_{k-1}} \rho\left(1, z, z^2\right)dz$$

2.3.2 Finite element formulation

The governing differential equation of tranverse vibration resposne of the various configurations of hybrid composite plates are formulated in finite element form by considering a rectangular plate element having nine nodes with five degrees of freedom (DOF) at each node. The DOF considered at each node are u_0, v_0, w_0, Ψ_x and Ψ_y where u_0 and v_0 are midplane displacements along x and y axes, respectively, w_0 is the transverse displacment along z axis and Ψ_x and Ψ_y are the bending rotations of the cross section at any point with respect to y and x directions of the plates, respectively. These displacments and bending rotations can be written in the form of nodal displacements and shape funcitons functions such that

$$\left\{\hat{u}\right\} = \begin{Bmatrix} \hat{u}_0 \\ \hat{v}_0 \\ \hat{w}_0 \\ \hat{\psi}_x \\ \hat{\psi}_y \end{Bmatrix} = [N]\{u\} \tag{25}$$

Where

$$[N] = \begin{bmatrix} N_i^u & 0 & 0 & 0 & 0 \\ 0 & N_i^v & 0 & 0 & 0 \\ 0 & 0 & N_i^w & 0 & 0 \\ 0 & 0 & 0 & N_i^{\psi_x} & 0 \\ 0 & 0 & 0 & 0 & N_i^{\psi_y} \end{bmatrix}. \tag{26}$$
$$\{u\} = \left\{u_{0i} \ \ v_{0i} \ \ w_{0i} \ \ \psi_{x_i} \ \ \psi_{x_i}\right\}^T, \ i = 1, 2, 3 \ldots 9$$

N_i is the standard shape function of u_{0_i}, v_{0_i}, w_{0_i}, Ψ_{x_i} and Ψ_{y_i}. Hamilton's principle is applied to nine node rectangular element of CNT reinforced hybrid composite plate to obtain the element equations of motion as follows

$$\left[M^e\right]\left\{\ddot{u}^e\right\} + \left[K^e\right]\left\{u^e\right\} = \left\{f^e\right\} \tag{27}$$

Where [M^e] and [K^e] are mass and stiffness matrices of the nine noded rectangular element, respectively and {f^e} is the element nodal force. System governing equations of motion of the CNT rienforced hybrid composite plate in matrix form is expressed by adopting finite element procedure.

$$[M]\left\{\ddot{u}\right\} + [K]\{u\} = \{f\} \tag{28}$$

where [M], [K], {u} and {f} are system mass, stiffness, degrees of freedom of the composite plate and dynamic loads, respectively.

The loss factor (η_i) at each mode is

$$\eta_i = \frac{\left\{\varphi_i^r\right\}^T\left[K^i\right]\left\{\varphi_i^r\right\}}{\left\{\varphi_i^r\right\}^T\left[K^r\right]\left\{\varphi_i^r\right\}} \tag{28}$$

3. Materials and experimental investigations

3.1 Materials

The materials used in this work are Carboxylic acid functionalized multi walled carbon with more than 95% chemical purity having the average dimensions of 17 nm diameter and 10 µm length. Further, they are randomly dispersed in low viscosity epoxy resin (LY556) with HY951 hardner and reinforced with E-glass fiber having 220 gsm.

3.2 Preparation of composite materials

Most polymers are either in a solid or viscous liquid state, which requires the polymer to be dissolved or diluted using a solvent to reduce the viscosity before dispersion of CNTs through ultrasonication process. When ultrasound propagates via a series of compression, attenuated waves are induced in the molecules of the medium through which it passes. The production of these shock waves promotes the "peeling off" of individual nanoparticles located at the outer part of the nanoparticle bundles, or agglomerates, and thus results in the separation of individualized nanoparticles from the bundles. If the sonication treatment is too aggressive and/or too long, CNTs can be easily and seriously damaged, especially when a probe sonicator is employed. However optimum time is to be chosen for sonication process. For some thermosetting polymers, such as epoxy, obvious CNT re agglomerations were observed after several hours of curing reaction. In order to overcome this, higher shear forces are applied through high speed shear mixer to achieve a fine dispersion in the polymer matrix.

The carboxylic acid (COOH) functionalized multi walled carbon nanotubes (MWCNTs) supplied by United Nanotech Innovations Private Limited® with more than 95% chemical purity having average dimensions of 17 nm outer diameter and 10 μm length were used. The MWCNT, as received, are highly intertwined with each other to form different sizes of aggregates. The individual MWCNT are indistinguishable from one another as shown in Fig. 3(a). This would be a barrier to the homogenous dispersion of MWCNT into the polymer matrix. In order to improve the performance of the CNT nanocomposites, CNT aggregates should be disintegrated into individual CNTs and disperse homogenously into the polymer matrix. High energy ultrasonic processing is applied to aggregate CNTs to disintegrate into individuals CNT which leads to better dispersion in the polymer matrix. Pre-calculated amounts of MWCNT were weighed in a container by using weighing machine to obtain required MCNT weight percentage in the hybrid composite. Initially, these MWCNT were mixed into the solvent by manual stirring for 2 minutes. Further a high intensity 12.5 mm probe ultrasonic processor was used to disintegrate the aggregate CNT's into solvent for an hour by using pulsed on–off mode 6s on /4s off. The beaker containing the mixture was placed in the ice bath to maintain working temperature of sonication process. A desired amount of Araldite L556 was first heated to 75℃ to reduce the viscosity and then added to CNT/solvent solution to obtain the required MWCNT/epoxy solution. This solution was further sonicated for 2 hours to effectively disperse the MWCNT in the low viscosity epoxy. This mixture was then placed in the oven at 70℃ for 48 hours to evaporate the solvent completely. Further, MWCNT/epoxy mixture was mixed for 30 mins by using shear mixer to ensure proper homogeneity of CNT into epoxy matrix.

The CNT-epoxy mixture which was prepared by Araldite LY556 resin and MWCNT was mixed with hardner HY951 with a ratio of 10:1 by weight. Fig. 3 shows the SEM image of pristine MWCNT, dispersed MWCNT after applying ultra-sonication to MWCNT/solvent mixture and CNT reinforced polymer composite. It is observed that the pristine CNT's are integrated into clusters, whereas the sonicated CNTs were better disintegrated into individuals. Further, Fig. 3(c) reveals the better dispersion of MWCNT in the epoxy matrix.

Fibers reinforced composite plates without and with CNT reinforcement were fabricated by using hand-layup technique. Initially peel ply was placed on the smooth flat surface to get smooth surface finish and release agent was then applied for easy removal of specimen. E-glass unidirectional fiber (92415) preform was placed over the smooth flat surface, and then mixture of MWCNT and Araldite LY556 was applied over the fiber by using the brush and roller. After layup process was completed, porous peel ply and bleeder were placed on top of the laminate stack. The complete layup was covered with vacuum bag, which was closed its periphery by a sealant. The laminate was then cured in two stages. In the first stage, the temperature was increased at control rate of 1℃/min up to 70℃ and in the second stage, dwelling at 70℃ for two hours. Further, the cured CNT reinforced hybrid composite plates were removed from the oven and allowed to cure at room temperature for an additional 24 h before they are cut into required dimensions. The same procedure was repeated to fabricate the GFRP composite plates without CNT reinforcement.

3.3 Mechanical characterization

3.3.1 Evaluation of flexural moduli

The complex moduli of the epoxy, MWCNT-epoxy, glass fiber polymer composite with and without reinforcement were evaluated using the Dynamic Mechanical Analyzer (DMA) at Central Institute of plastic Engineering and Technology (CPIET), Chennai. Polymer composite with 1 wt% of MWCNT reinforcement and a unidirectional GFRP composites with 0.5wt% of CNT reinforcement of rectangular cross section 80 mm × 13 mm × 3 mm with ply orientations $[0°]_{10}$ and $[90°]_{10}$ were fabricated using vacuum assisted hand lay-up process as explained in section 3.2. The glass fiber volume fraction was found to be 0.34 for the

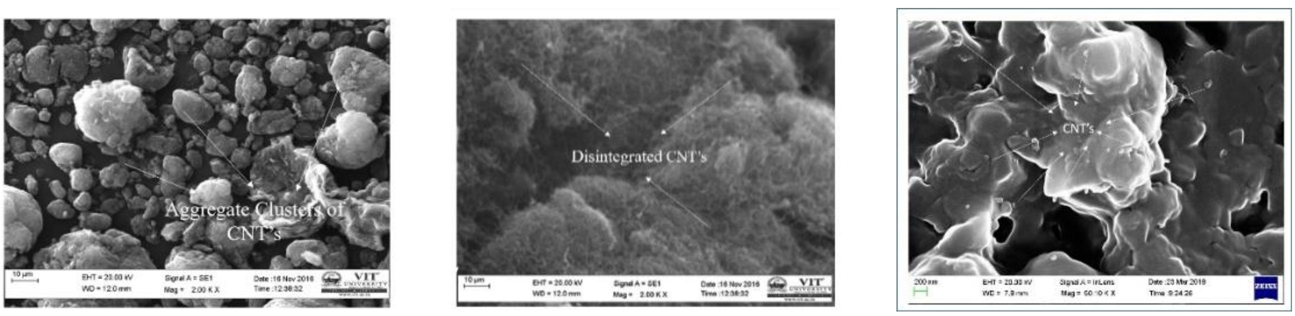

(a) As received MWCNT (b) Solvent free sonicated MWCNT (c) MWCNT/Epoxy composite

Fig. 3 SEM images of hybrid composites

Table 1 The various mechanical properties of composites with and without CNT reinforcement

Properties	Epoxy	Epoxy with 1wt% of CNT	GFRP lamina	CNT-GFRP lamina
v_f	-	-	0.343	0.341
E_{11} (GPa)	3.45(1+j0.035)	4.05(1+j0.0567)	25.58(1+j0.014)	26.01(1+j0.0185)
E_{22} (GPa)	3.45(1+j0.035)	4.05(1+j0.0567)	5.39(1+j0.0152)	5.95(1+j0.0202)
G_{12} (GPa)	1.33(1+j0.011)	1.48(1+j0.0181)	1.89(1+j0.0072)	2.1(1+j0.0102)

CNT hybrid composite. ASTM D5418 standard was followed to perform the dual cantilever flexural test. The strain is applied at the midway of the dual cantilever beam to measure elastic and loss modulus in real time using the computer running data acquisition and analysis software. The measured complex moduli are presented in Table 1.

3.3.2 Evaluation of shear moduli and Poisson's ratio

The shear modulus (G_{12}) of the epoxy, CNT-epoxy, glass fiber polymer composite with and without CNT reinforcement were measured in terms of storage and loss modulus using strain controlled rheometer (Anton Paar Physica MCR 301) available at IIT Kharagpur. A rectangular specimen of 76 mm × 13 mm × 2 mm was tested in dynamic torsion mode using ASTM D5279. Dynamic mechanical testing determines the thermo mechanical characteristics by measuring the storage modulus and loss moduli as a function of temperature. The measured shear moduli (G_{12}) of various composites are presented in Table 1.

4. Validation of finite element formulation

The competence of developed finite element formulation in diagnosing the dynamic properties of CNT reinforced hybrid composite is verified by comparing the experimental natural frequencies of GFRP composite plates with and without CNT reinforcement. Fiber reinforced composite plates without and with CNT reinforcement measuring 420 × 250 × 3.7 mm were fabricated by using hand-layup technique as mentioned in section 3.2. All the fabricated composite specimens were then cut into 400 mm × 200 mm × 3.7 mm by using zig saw and are as shown in Figs. 4 and 5.

The ply orientation of C0, C1, C2 and C3 configurations of hybrid GFRP composite plate were considered as $[0°/90°]_{4s}$ at left end and $[0°/90°]_{2s}$, $[0°/90°]_{2s}$ and $[0°]_{4s}$ at right end with 0.23 mm, 0.225 mm, 0.23 mm and 0.24 mm ply thickness, CNT wt% of 0.5, 0.4, 0.5 and 0.44 and glass fiber volume fraction of 0.34, 0.4, 0.34 and 0.3, respectively. The same ply orientations were considered to fabricate C0, C1, C2 and C3 configurations of GFRP composite without CNT reinforcement with thickness of each ply is 0.23 mm and fiber volume fraction of 0.34, 0.35, 0.33 and 0.33, respectively. The block diagram and experimental setup used to perform the experimental investigations on GFRP composite plate with and without CNT reinforcement is shown in Fig. 6. Roving hammer (Impulse Force Hammer-086C03) was used to accelerate all the configurations of composite plate and z-axis oriented accelerometer was attached on the top surface of the GFRP with and without CNT reinforcement composite plates to measure the acceleration due to induced excitation. These transverse acceleration signals were converted into frequency response function by using four channel Data Acquisition system (Model no: ATA − D AQ042451). The natural frequencies of the plates were spotted from the peaks in the frequency response diagram.

The validity of developed FEM for the different configurations of GFRP laminated composite plate with and

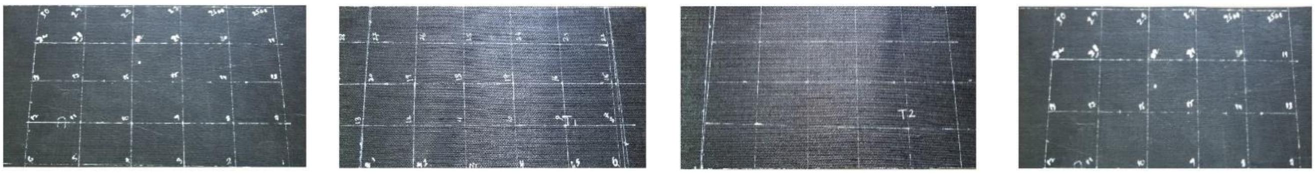

(a) C0 Configuration (b) C1 Configuration (c) C2 Configuration (d) C3 Configuration

Fig. 4 Photographs of uniform and various tapered configurations of CNT hybrid GFRPC plates

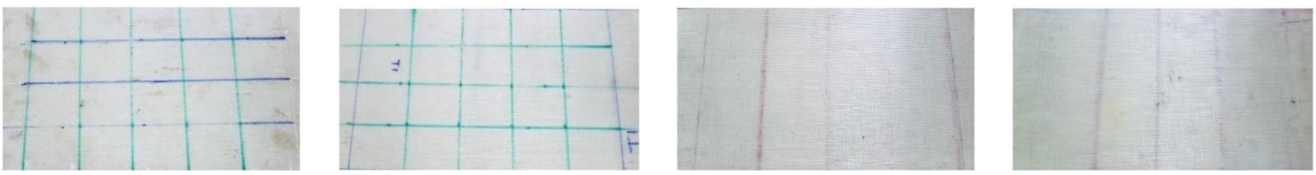

(a) C0 Configuration (b) C1 Configuration (c) C2 Configuration (d) C3 Configuration

Fig. 5 Photographs of uniform and various tapered configurations of GFRPC plates

Table 2 Mechanical properties of different configurations of composite fiber lamina, CNT, Glass fiber and epoxy matrix

Properties	GFRP composite lamina			CNT-hybrid Composite lamina		
	C0	C1	C2, C3	C0, C2	C1	C3
v_f	0.34	0.35	0.33	0.34	0.4	0.3
E_{11} $(1+j\eta)$ (GPa)	25.6(1+j 0.014)	26.3(1+ j 0.0139)	25.1(1+ j 0.014)	26.01(1+ j 0.018)	30.0(1+ j 0.017)	23.54(1+ j 0.019)
E_{22} $(1+j\eta)$ (GPa)	5.4(1+j 0.015)	5.4(1+ j 0.0148)	5.2(1+ j 0.015)	5.95(1+ j 0.202)	6.2(1+ j 0.019)	5.85(1+ j 0.020)
υ_{12}	0.273	0.272	0.274	0.292	0.287	0.295
G_{12} $(1+j\eta)$ (GPa)	1.9(1+j 0.007)	1.9(1+ j 0.0071)	1.9(1+ j 0.007)	2.10(1+ j 0.011)	2.31(1+ j 0.010)	2.01(1+ j 0.011)
G_{23} $(1+j\eta)$ (GPa)	2.1(1+ j 0.006)	2.1(1+0. j 0060)	2.1(1+ j 0.006)	2.30(1+ j 0.008)	2.40(1+ j 0.008)	2.21(1+ j 0.009)
ρ (kg/m^3)	1656	1669	1642	1660	1740	1606

Table 3 Comparison of natural frequencies evaluated using present FEM with the experimental measured frequencies under CFCF boundary condition

Type of composite	Modes (m,n)	Natural Frequencies (Hz)											
		C0		C1		C2		C3		% deviation			
		FEM	EXP	FEM	EXP	FEM	EXP	FEM	EXP	C0	C1	C2	C3
GFRP composite	(1,1)	137.45	129.11	110.16	102.67	110.49	106.77	120.18	116.01	6.06	6.79	3.36	3.46
	(1,2)	155.68	148.17	125.14	122.34	125.33	125.31	133.47	137.32	4.82	2.23	0.01	-2.88
	(2,1)	340.56	343.42	268.88	269.31	266.31	264	221.45	236.84	-0.01	-0.15	0.86	-6.49
	(1,3)	380.32	381.3	305.51	287.5	305.16	306.33	334.1	329.18	-0.25	5.89	-0.38	1.47
	(2,2)	405.71	399.72	325.9	311.39	325.41	317.19	351.96	344.03	1.47	4.45	2.52	2.25
	(2,3)	553.27	548.2	443.81	443.38	441.57	442.49	433.49	427.27	1.01	0.09	-0.20	1.43
CNT reinforced hybrid composite	(1,1)	139.77	131.32	113.45	106.09	112.98	112.25	124.78	125.45	6.04	6.48	0.65	-0.53
	(1,2)	160.5	158.48	130.15	129.88	129.84	129.92	140.74	152.25	1.25	0.20	-6.16	-8.17
	(2,1)	352.55	356.45	280.61	272.4	277.41	278.71	242.28	252.18	-1.10	2.92	-0.46	-4.08
	(1,3)	387.14	385.51	314.87	306.5	312.27	308.21	346.91	331.67	0 .42	2.65	1.3	4.39
	(2,2)	416.15	425.82	337.67	356.23	335.37	356.18	368.5	368.72	-2.32	-5.41	-6.20	-0.05
	(2,3)	574.39	618.54	463.79	453.5	460.52	463.8	464.37	439.74	-7.68	6.02	-0.71	5.3

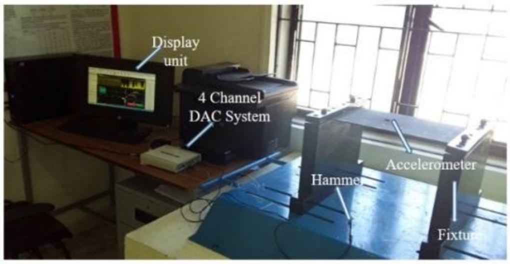

(a) Photograph of Experimental setup

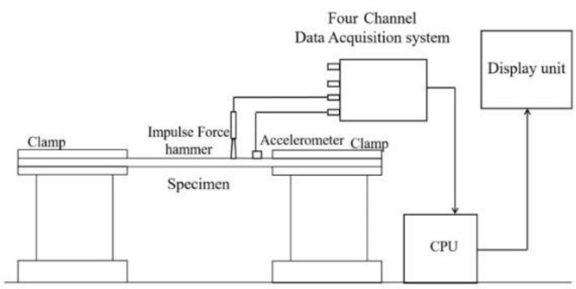

(b) Block diagram of the experimental setup

Fig. 6 Experimental setup

without CNT is performed by comparing the experimentally measured natural frequencies with those calculated from FEM. The complex elastic moduli of different configurations of composite fiber lamina, CNT, Glass fiber and epoxy matrix were derived based on a correspondence principle using analytical expression given in Eq. (1)-(11) are presented in Table 2. Experiments were performed under clamped (C) at both thick and thin ends of the plate and free (F) at all other ends (CFCF). The simulation and experimental natural frequencies are acquired based on the modes considered along longitudinal direction (m) and transverse direction (n) corresponding to the mode shapes (m,n) of composite plates. The lowest six natural frequencies of the various composite plate were compared for the various modes (1,1), (1,2), (2,1), (1,3) (2,2) and (3, 1) under CFCF end conditions for the configurations C0, C1, C2 and C3 as reported in Table 3. The natural frequencies derived from the numerical simulations have very close agreement with experimentally measured frequencies for all the configurations of composite plates without and with CNT reinforcement. The deviation of FEM results with the experimental values is due to deviation of actual volume fraction of glass fiber and CNT,

Table 4 Comparison of damping ratio evaluated using present FEM with the experimental measured values under CFCF boundary condition

Type of composite	Modes (*m*,*n*)	Damping ratio											
		C0		C1		C2		C3		% deviation			
		FEM	EXP	FEM	EXP	FEM	EXP	FEM	EXP	C0	C1	C2	C3
GFRP composite	(1,1)	0.00735	0.0079	0.0074	0.007	0.0074	0.0071	0.0077	0.0069	-7.08	5.03	4.18	10.25
	(1,2)	0.00638	0.007	0.0064	0.0062	0.0065	0.0061	0.0069	0.0066	-9.25	3.42	5.26	5.07
	(2,1)	0.00649	0.0067	0.0065	0.0064	0.0065	0.0068	0.0065	0.0071	-2.84	2.61	-4.15	-9.61
	(1,3)	0.00722	0.0071	0.0073	0.0075	0.0073	0.0079	0.0076	0.0073	1.83	-2.34	-7.51	4.86
	(2,2)	0.00671	0.0063	0.0068	0.0072	0.0068	0.0061	0.0072	0.0069	6.00	-6.48	10.4	4.99
	(2,3)	0.00616	0.0057	0.0062	0.0056	0.0062	0.0058	0.0065	0.0061	8.83	10.47	6.28	6.13
CNT reinforced hybrid composite	(1,1)	0.00927	0.0088	0.0091	0.01	0.0093	0.009	0.011	0.0098	5.10	-9.89	3.12	10.67
	(1,2)	0.00836	0.0074	0.0081	0.0078	0.0084	0.0079	0.0084	0.0076	12.52	3.70	5.95	9.74
	(2,1)	0.00864	0.0083	0.0084	0.0092	0.0087	0.0082	0.0085	0.0079	4.60	-10.18	5.78	7.06
	(1,3)	0.00916	0.009	0.0089	0.0084	0.0092	0.009	0.01	0.0089	2.35	5.83	2.38	11.18
	(2,2)	0.00867	0.008	0.0084	0.0079	0.0087	0.0081	0.0091	0.0082	8.78	6.40	6.98	9.89
	(2,3)	0.00821	0.0077	0.008	0.0082	0.0083	0.0086	0.008	0.0071	6.26	-2.89	-3.51	11.03

Table 5 Comparison of the natural frequencies of the different configurations of a tapered composite plate derived by using the present FEM with those presented in Sudhagar *et al*. (2015)

Modes (*m*,*n*)	Natural frequencies (Hz)											
	C0		C1		C2		C3		% deviation			
	Sudagar *et al*. (2015)	Present	Sudagar *et al*. (2015)	Present	Sudagar *et al*. (2015)	Present	Sudagar *et al*. (2015)	Present	C0	C1	C2	C3
(1,1)	37.16	37.024	40.77	41.043	41.64	41.639	43.7	44.631	0.37	0.67	0.00	2.1
(1,2)	67.36	65.497	62.15	61.852	62.98	61.675	62.9	63.069	2.77	0.48	2.07	0.27
(2,1)	230.97	229.27	199.44	200.77	202.61	207.52	224.7	228.54	0.74	0.67	2.42	1.71
(2,2)	278.76	274	226.77	227.51	229.89	232.9	246.5	249.77	1.71	0.33	1.31	1.33
(1,3)	250.9	248.33	173.82	177.71	174.44	164.62	137.2	137.98	1.02	2.24	5.63	0.57
(3,1)	651.25	642.48	-	519.3	535.01	540.03	590.3	597.54	1.35	-	0.94	1.23

mechanical properties of composite lamina with the measured values and manufacturing defects. Based on the experimental results, it is evident that the bending natural frequencies of CNT reinforced hybrid composite plates under CFCF end conditions at all modes increase with addition of MWCNT's into composite plate. It can be observed that the fundamental natural frequencies of C1, C2 and C3 configurations of CNT reinforced composite plates could be increased approximately 3.33%, 5.36% and 8.13% with addition of MWCNT wt% of 0.4, 0.5 and 0.44 respectively, compared to those of composite plates without MWCNT reinforcement under CFCF end condition. This is attributed due to the presence of MWCNT in composite which restricts the motion of the polymer chains which consequently improves the bending stiffness of the MWCNT reinforced hybrid composite plate than that of laminated composite plate without MWCNT reinforcement. The natural frequencies of C0 configuration of hybrid composite plate for (1, 1) and (1, 2) modes are increasing less than 1% as comparing with the laminated composite without CNT reinforcement. This could be due to the week bonding between glass fiber and MWCNT/epoxy matrix.

Further, the validity of developed FEM for the different configurations of GFRP laminated composite plate with and without MWCNT is performed by comparing the experimentally measured damping ratio with those calculated from FEM. The damping ratios of various configurations of GFRP laminated composite plate with and and without MWCNT reinforcement for the lowest six modes under CFCF mode are presented in Table 4. It is observed that the damping ratio of various configurations of GFRP laminated composite plate increases at all the modes compared with those of GFRP composite plate without CNT reinforcement. Further, it was noticed that the fundamental damping ratio of C0, C1, C2 and C3 configuration of MWCNT reinforced composite plates could be increased approximately 10.3%, 37.9%, 26.7% and 36.1% with addition of MWCNT wt% of 0.5, 0.4, 0.5 and 0.44 respectively compared to those of composite plates without CNT reinforcement under CFCF boundary condition. This is because of the improved dissipative energy of composite plates in each cycle of oscillation due

Table 6 Effect of volume fraction of MWCNT on the natural frequencies (Hz) of MWCNT reinforced hybrid laminate composite plate with various configurations

Type of composite	Modes (m,n)	Volume fraction (v_{CNT} in %)					
		0	0.5	1	1.5	2.0	2.5
C0	(1,1)	137.34	140.82	143.21	144.5	144.83	144.43
	(1,2)	155.57	162.42	167.12	169.75	170.59	170.07
	(2,1)	380.02	390.18	397.08	400.82	401.79	400.66
	(2,2)	405.42	420.44	430.7	436.39	438.09	436.8
	(1,3)	340.34	357.23	368.8	375.29	377.38	376.17
	(3,1)	749.01	770.39	784.81	792.61	794.68	792.43
C1	(1,1)	108.94	111.67	113.54	114.55	114.79	114.44
	(1,2)	124.03	129.52	133.28	135.36	136.01	135.56
	(2,1)	300.26	307.95	313.19	315.99	316.66	315.71
	(2,2)	320.89	332.49	340.42	344.78	346.03	344.93
	(1,3)	267.47	281.05	290.32	295.49	297.12	296.09
	(3,1)	581.6	596.98	607.38	612.96	614.3	612.44
C2	(1,1)	111.33	113.98	115.79	116.75	116.97	116.89
	(1,2)	126.16	131.54	135.22	137.27	137.89	137.59
	(2,1)	307.46	315.12	320.31	323.08	323.72	323.47
	(2,2)	327.68	339.21	347.07	351.38	352.6	352.04
	(1,3)	267.96	281.53	290.8	295.96	297.59	296.79
	(3,1)	598.97	614.6	625.11	630.71	632.04	631.52
C3	(1,1)	121.99	123.99	125.69	126.03	126.13	125.79
	(1,2)	135.21	139.79	143.78	144.65	145.14	144.7
	(2,1)	339.08	344.94	349.85	350.82	351.13	350.16
	(2,2)	356.85	366.32	374.46	376.19	377.05	375.96
	(1,3)	223.32	240.59	255.38	258.7	260.87	259.84
	(3,1)	662.6	674.99	685.23	687.26	687.96	686.06

to the slippage action between the MWCNT and the polymer matrix.

5. Parametric study

The dynamic properties of the CNT reinforced hybrid laminate composite are remarkably affected by the material and geometrical properties. These properties are further influenced by configurations of composite plate, volume fraction of CNT, aspect ratio of CNT. Hence, a parametric study has been performed to investigate the effect of all those parameters on dynamic properties of CNT reinforced hybrid laminate composite using the developed finite element formulation. The geometrical properties considered for all the configurations of hybrid composite lamina are length (L) 300 mm, Width (B) 200 mm and ply thickness of 0.23 mm. The ply orientations of composite plate considered for the simulation are $[0°/90°]_{4s}$ at right end and $[0°/90°]_{4s}$, $[0°/90°]_{2s}$, $[0°/90°]_{2s}$ and $[0°]_{4s}$ at left end for C0, C1, C2 and C3, respectively. Uniform thickness is obtained for C0 configuration by maintaining same ply orientations at right end without dropping any plies. Taper configurations are obtained by dropping continuous piles in and C2 and alternate plies in C3. Taper angle considered for the tapered configurations of C1, C2 and C3 of the hybrid composite plate is 0.175°. Volume fraction of glass fiber and CNT are assumed to be identical for all the configurations and equal to 0.34. The weight percentage (wt%) and aspect ratio of MWCNT are considered to be 0.5 and 578, respectively. The material properties of CNT hybrid composite plate and CNT/epoxy considered for numerical simulations are presented in Table 1.

5.1 Effect of volume fraction of CNT on natural frequencies and loss factor

The effect of volume fraction of MWCNT on natural frequencies of the various configurations of MWCNT reinforced hybrid laminated composite plate are studied by considering the volume fractions of CNTs varying from 0 to 2.5% and the results are presented in Table 6. The natural frequencies tend to increase at all the modes with the increase in volume fraction of MWCNT from 0 to 2%. This can be related to the fact that the CNT's in epoxy matrix restricts the mobility of polymer chains which improves the stiffness and strength of the composite. The rate of

Table 7 Effect of Volume fraction of MWCNT on the loss factor of MWCNT reinforced hybrid laminate composite plate with various configurations

Type of composite	Modes (m,n)	Volume fraction (v_{CNT} in %)			
		0.5	1.0	1.5	2.0
C0	(1,1)	0.019369	0.021403	0.021415	0.020826
	(1,2)	0.014174	0.016092	0.016767	0.01442
	(2,1)	0.019256	0.021289	0.021309	0.020723
	(2,2)	0.016154	0.017995	0.018373	0.016608
	(1,3)	0.019065	0.021017	0.021088	0.020015
	(3,1)	0.018849	0.021016	0.021091	0.020465
C1	(1,1)	0.020036	0.022294	0.022291	0.021554
	(1,2)	0.014704	0.0166	0.017227	0.014879
	(2,1)	0.019733	0.021923	0.02193	0.021263
	(2,2)	0.017028	0.018952	0.019248	0.017596
	(1,3)	0.018548	0.020518	0.020679	0.01927
	(3,1)	0.017712	0.020924	0.021432	0.020767
C2	(1,1)	0.019381	0.021423	0.021434	0.020856
	(1,2)	0.014417	0.016277	0.016907	0.014584
	(2,1)	0.019295	0.021341	0.021357	0.020797
	(2,2)	0.016742	0.018587	0.018889	0.017308
	(1,3)	0.018391	0.020315	0.020478	0.019073
	(3,1)	0.017198	0.019843	0.020715	0.020138
C3	(1,1)	0.021145	0.023896	0.023869	0.023095
	(1,2)	0.015764	0.017745	0.0183	0.016076
	(2,1)	0.02015	0.022651	0.022669	0.022065
	(2,2)	0.020017	0.022004	0.022178	0.019475
	(1,3)	0.018005	0.020134	0.020352	0.018918
	(3,1)	0.018356	0.020514	0.020809	0.018422

increasing in the natural frequencies lowers with the increase of the volume fraction of MWCNT due to aggregates of CNT into the epoxy. Further increasing in the volume fraction of CNT from 2% to 2.5% decreases the natural frequencies of hybrid composite. This can be attributed to the reduction in stiffness of composite due to the reduction in the load transfer capacity to CNT's with formation of clusters at higher volume fraction of CNT (> 2%). Further, it is observed that the natural frequencies decreases in the order of C0, C3, C2, C1 for the modes such as (1, 1), (1, 2), (2, 1), (2, 2) and (3, 1) at same volume fraction . The natural frequencies decreases in the order of C0, C2, C1 and C3 for other modes such as (1, 3) modes at same volume fraction. It can be noted that the ply orientations at right end of the plate is $[0^o/90^o]_{4s}$ in C0 configuration which results the highest stiffness relative to C3, C1 and C2 with $[0°]_{4s}$, $[0°/90°]_{2s}$ and $[0°/90°]_{2s}$ ply orientations, respectively. Since all the plies in C3 are orientated at 0°, C3 exhibit the highest stiffness in longitudinal direction compared to that of C1 and C2 configurations. Even though the ply orientations are same for C2 and C1, the location of resin pockets are in low bending stress regions close to mid plane surface of the composite results higher stiffness for C2 comparing with C1 configuration. Hence the stiffness decreases in the order of C0, C3, C2 and C1 along the longitudinal direction which causes decreasing in natural frequencies in same order at (1, 1), (2, 1), (2, 2) and (3, 1) modes.

The effect of volume fraction of CNT on loss factor of the various configurations of MWCNT reinforced hybrid laminated composite plate are studied by considering the volume fractions of CNTs by varying from 0.5 to 2% and the results are presented in Table 7. The loss factor tend to increase at all the modes with the increase in volume fraction of MWCNT from 0.5% to 1.5%. This could be due to the stick slip mechanism between graphene layer and interfacial sliding at the CNT-matrix region of the composite plate. Further increasing in the volume fraction of CNT from 1.5% to 2% decreases the loss factor of hybrid composite. This can be attributed to the reduction in frictional energy dissipation of composite with the reduced sliding at the MWCNT- polymer interface due to formation of clusters at higher volume fraction of CNT (≥ 2%). It is also seen that the loss factor increases in the order of C0, C2, C1 and C3 for the all the modes except for the modes (1, 3) and (3, 1) at same volume fraction.

Table 8 Effect of aspect ratio of MWCNT on the natural frequencies (Hz) of CNT reinforced hybrid laminate composite plate with various configurations under CFFF boundary condition

Configuration	Modes (m,n)	Aspect ratio (l/d)				
		100	500	1000	1500	2000
C0	(1,1)	21.713	21.892	21.938	21.956	21.966
	(1,2)	47.686	48.885	49.193	49.312	49.376
	(2,1)	136.18	137.31	137.61	137.72	137.78
	(2,2)	181.92	185.31	186.18	186.52	186.7
	(1,3)	287.17	291	291.99	292.37	292.58
	(3,1)	381.66	385.37	386.31	386.67	386.86
C1	(1,1)	23.867	24.076	24.131	24.152	24.163
	(1,2)	44.298	45.402	45.686	45.796	45.855
	(2,1)	117.4	118.39	118.64	118.74	118.79
	(2,2)	147.56	150.09	150.75	151	151.14
	(1,3)	195.92	199.11	199.93	200.25	200.42
	(3,1)	308.03	311.38	312.36	312.75	312.97
C2	(1,1)	24.595	24.793	24.845	24.865	24.875
	(1,2)	44.766	45.857	46.138	46.247	46.305
	(2,1)	119.91	120.86	121.1	121.2	121.25
	(2,2)	149.53	152.01	152.65	152.9	153.03
	(1,3)	194.46	197.65	198.48	198.8	198.97
	(3,1)	313.64	316.47	317.24	317.54	317.7
C3	(1,1)	25.562	25.73	25.774	25.791	25.8
	(1,2)	44.439	45.489	45.76	45.865	45.92
	(2,1)	130.1	131.02	131.24	131.33	131.38
	(2,2)	157.11	159.3	159.87	160.09	160.21
	(1,3)	143.63	148.2	149.39	149.85	150.1
	(3,1)	345.45	347.47	347.99	348.2	348.31

5.2 Effect of aspect ratio of CNT on natural frequencies

The effect of aspect ratio of CNT on the natural frequencies of C0, C1, C2 and C3 configurations of CNT reinforced composite plate under CFFF boundary condition are investigated by performing numerical simulation and the results are presented in Table 8. The natural frequencies for all the configurations increase insignificantly with the increase of aspect ratio of CNT. This could be due to poor load transfer between the adjacent CNT's for the randomly distributed CNT's as compared with the aligned CNT's. Similar observations were also reported in Ashrafi and Hubert (2006). This results in negligible improvement in the stress transfer to CNT's from epoxy matrix with the increase in aspect ratio of CNT. Further with the increase in aspect ratio, CNT's are prone to form aggregates due to the cotton like structure of the long CNT's. It is also seen that the natural frequencies increase in the order of C0, C1, C2 and C3 at all the modes except at (1, 1) and (1, 3) modes under CFFF boundary condition.

5.3 Effect of MWCNT on transverse vibration response

The effect of CNT reinforcement on the transverse vibration response of GFRP composite plate with and without CNT reinforcement is studied using various configurations with $[0°/90°]_{4s}$ ply orientations, and 0.5wt% of MWCNT under CFFF boundary condition by considering harmonic excitation force of magnitude 5 N at distance of 100 × 100 mm from left end corner of the plate. Forced vibration simulation is performed on various configurations of GFRP composite plate with and without MWCNT reinforcement to determine the root mean square velocity spectrum. Fig. 8 shows the response spectrum over the excitation frequency range of 1-250 Hz under CFFF boundary condition. It is noticed that the mean square velocity spectrum of GFRP composite plate without MWCNT reinforcement is higher than the CNT reinforced hybrid composite plate under CFFF condition. This is due to the enhancement of stiffness of MWCNT reinforced hybrid composite plate and consequently the load carrying capacity of hybrid composite structure could be increased.

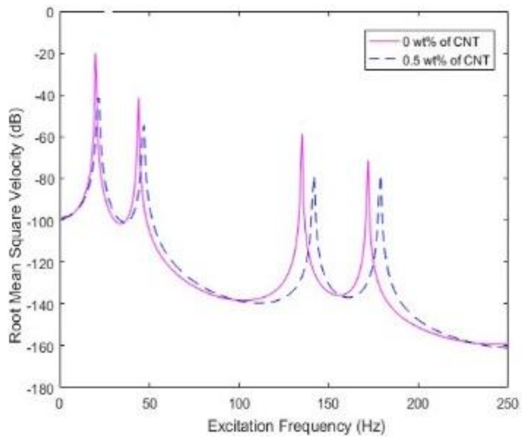

(a) C0 Configuration

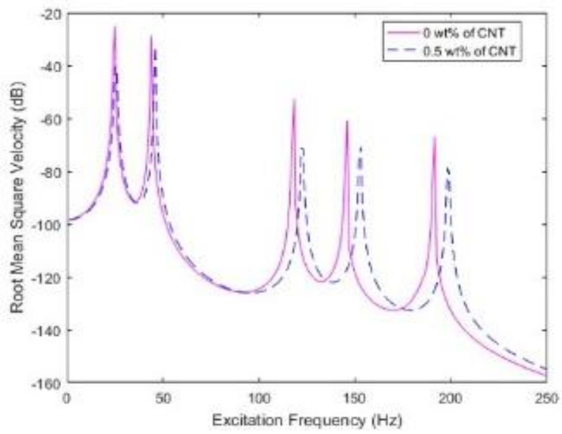

(b) C1 Configuration

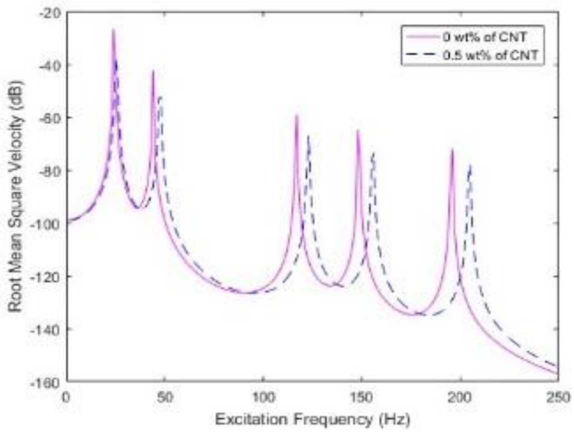

(c) C2 Configuration

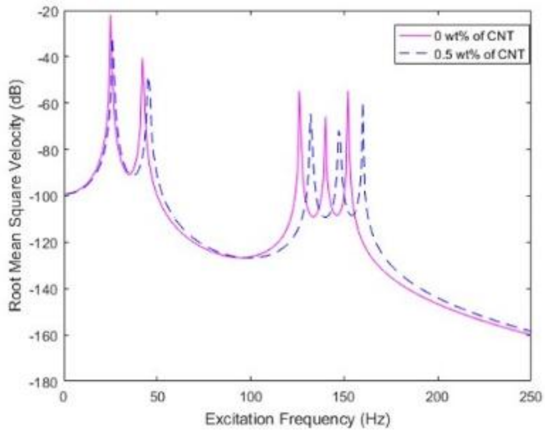

(d) C3 Configuration

Fig. 8 Transverse vibration responses of GFRP composite plate with and without MWCNT reinforcement under CFFF boundary condition

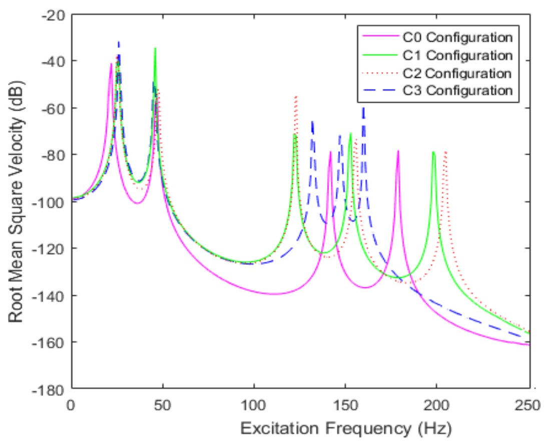

Fig. 9 Transverse vibration responses of various configurations with 0.5 wt% of MWCNT reinforced GFRP composite plates under CFFF boundary condition

Further the forced vibration simulation is performed on different configurations of the hybrid tapered composite plates with identical CNT content of 0.5wt%. Fig. 9 shows the response spectrum over the excitation frequency range of 1-250 Hz under CFFF boundary condition. It is noticed that the mean square velocity spectrum of the tapered configurations increases in the order of C2, C1 and C3 under CFFF boundary condition. This could be due to the location of resin pockets and number of ply drops of composite plate. The results also confirm that the transient vibration amplitude can be altered with different configurations of hybrid composite plate. This is because of variation of stiffness and mass along the longitudinal direction of the composite plates. Hence it is understood that the stiffness and flexibility of the CNT hybrid composite is significantly altered by changing the location of resin pockets and the configuration of plates in addition to the enhancement of stiffness of the structure without any significant change in mass.

6. Conclusions

In the present study, the free and forced vibration responses of MWCNT embedded fiber reinforced polymer uniform and tapered composite (MWCNT-FRP) plates are investigated numerically and experimentally. The governing equations of motion of FRP composite plates without and with MWCNT reinforcement were derived by considering a nine- node rectangular elements with five degrees of freedom (DOF) at each node. The effectiveness of the developed finite element formulation was demonstrated by comparing the natural frequenices of FRP composite plates without and with MWCNT reinforcemnt obtained experimentally. Various parametric studies are also performed to study the effect of CNT volume fraction, CNT aspect ratio, on the natural frequencies of different tapered configurations of MWCNT reinforced hybrid composite plates. It was observed that the fundamental natural frequency of the 0.5wt% MWCNT-GFRP hybrid composite plate is approximately 9% higher than that of GFRP composite plate without CNT reinforcement under CFCF boundary condition. The natural frequencies of CNT-GFRP hybrid composite plates tend to decrease with the increase of CNT volume fraction beyond 2% due to agglomeration of CNT's. It is also observed that the aspect ratio of the CNT have negligible effect on the improvement of dynamics properties due to randomly orientation of CNT's. Further the forced vibration analysis is performed to compare the dynamic response of the various configurations of CNT-GFRP composite plate with GFRP composite plate under harmonic excitations.

It was observed that the fundamental natural frequencies of MWCNT reinforced tapered hybrid composite plates (C1, C2 and C3 configurations) are higher in the order of 3.33%, 5.36% and 8.13%, respectively, compared to those of composite plates without MWCNT reinforcement under CFCF end condition. It was also noticed experimentally that the fundamental damping ratio of C0, C1, C2 and C3 configuration of GFRP composite plates could be increased approximately 10.3%, 37.9%, 26.7% and 36.1% with addition of MWCNT wt% of 0.5, 0.4, 0.5 and 0.44 respectively under CFCF boundary condition. It is understood that the presence of CNT not only improves the stiffness of the composite by restricting motion of the polymer chain but also improves the damping capability due to interfacing sliding of MWCNT and epoxy. A saturation limit on increment in natural frequencies of the hybrid composite structures was also observed at 2 Vol% MWCNT reinforcement. This will provide a platform for the designer to identify the optimal volume fraction of CNTs to be reinforced in the structure.

Acknowledgments

Authors are grateful to Science and Engineering Research Board (SERB), Department of Science and Technology, Government of India, for providing financial support through the project entitled 'A study of Structural damping and forced vibration responses of carbon nanotube Reinforced rotating Tapered Hybrid composite plates" under the Grant No. SR/FTP/ETA-0009/2014 to carry out this work.

References

Ashrafi, B. and Hubert, P. (2006), "Modeling the elastic properties of carbon nanotube array/polymer composites", *Compos. Sci. Techno.l*, **66**(3-4), 387-396.

Bai, J.B. and Allaoui, A. (2003), "Effect of the length and the aggregate size of MWNTs on the improvement efficiency of the mechanical and electrical properties of nanocomposites—experimental investigation", *Compos.: Part A: Appl. Sci. Manuf.*, **34**(8), 689-694.

Dai R.L. and Liao, W.H. (2009), "Fabrication, Testing, and Modeling of Carbon Nanotube Composites for Vibration Damping", *J. Vib. Acoust.*, **131**(5), 051004-1-051004-9.

DeValve, C. and Pitchumani, R. (2013), "Experimental investigation of the damping enhancement in fiber-reinforced composites with carbon nanotubes", *Carbon*, **63**, 71-83.

Formica, G., Lacarbonara, W. and Alessi, R. (2010), "Vibrations of carbon nanotube-reinforced composites", *J. Sound Vib.*, **329**(10), 1875-1889.

Gong, X., Liu, J., Baskaran, S., Voise, R.D. and Young, J.S. (2000), "Surfactant-assisted processing of carbon nanotube/ polymer composites", *Chem. Mater.*, **12**(4) 1049-1052.

Hashin, Z. (1970), "Complex modulus of viscoelastic composites-II. Fiber Reinforced Materials", *Int. J. Solids Struct.*, **6**(6), 797-807.

Jakkamputi, L.P. and Rajamohan, V. (2017), "Dynamic characterization of CNT-reinforced hybrid polymer composite beam under elevated temperature—an experimental study", *Polym. Compos.* DOI: 10.1002/pc

Khan, S.U., Li, C.Y., Siddiqui, N.A. and Kim, J.K. (2011), "Vibration damping characteristics of carbon fiber-reinforced composites containing multi-walled carbon nanotubes", *Compos. Sci. Technol.*, **71**(12), 1486-1494.

Lau, K.T. (2003), "Interfacial bonding characteristics of nanotube/polymer composites", *Chem. Phys. Lett.*, **370**(3-4) 399-405.

Lei, Z.X., Liew, K.M. and Yu, J.L. (2013), "Free vibration analysis of functionally graded carbon nanotube-reinforced composite plates using the element-free kp-Ritz method in thermal environment", *Compos. Struct.*, **106**, 128-138.

Mallick, P.K. (2007), *Fiber Reinforced Composites*, CRC Press, Boca Raton, FL, USA.

Montazeri, A. and Montazeri, N. (2011), "Viscoelastic and mechanical properties of multi walled carbon nanotube/epoxy composites with different nanotube content", *Mater. Des.*, **32**(4), 2301-2307.

Montazeri, A., Javadpour, J., Khavandi, A., Tcharkhtchi, A. and Mohajeri, A. (2010), "Mechanical properties of multi-walled carbon nanotube/epoxy composites", *Mater. Des.*, **31**(9), 4202-4208.

Omidi, M., Rokni, D.T.H., Milani, A.S., Seethaler, R.J. and Arasteh, R. (2010), "Prediction of the mechanical characteristics of multi-walled carbon nanotube/epoxy composites using a new form of the rule of mixtures", *Carbon*, **48**(11), 3218-3228.

Qian, D., Dickey, E.C., Andrews, R. and Rantell, T. (2000), "Load transfer and deformation mechanisms in carbon nanotube polystyrene composites", *Appl. Phys. Lett.*, **76**(20), 2868-2870.

Rafiee, M., Nitzsche, F. and Labrosse, M.R. (2018), "Effect of functionalization of carbon nanotubes on vibration and damping characteristics of epoxy nanocomposites", *Polym. Test.* DOI: 10.1016/j.polymertesting.2018.05. 037

Rajoria, H. and Jalili, N. (2005), "Passive vibration damping enhancement using carbon nanotube-epoxy reinforced composites", *Compos. Sci. Technol.*, **65**(14), 2079-2093.

Sudhagar, P.E., Babu, A.A., Vasudevan, R. and Jeyaraj, P. (2015), "Vibration analysis of a tapered laminated thick composite plate with ply drop-offs", *Arch. Appl. Mech.*, **85**(7), 969-990.

Thostenson, E.T. and Chou, T.W. (2003), "On the elastic properties of carbon nanotube-based composites: modelling and characterization", *J. Phys. D: Appl. Phys.*, **36**(5), 573-582.

Thostenson, E.T., Ren, Z. and Chou, T.W. (2001), "Advances in the science and technology of carbon nanotubes and their composites: a review", *Compos. Sci. Technol.*, **61**(13) 1899-

1912.
Wang, M., Li, Z.M. and Qiao, P. (2018), "Vibration analysis of sandwich plates with carbon nanotube-reinforced composite face-sheets", *Compos. Struct.* DOI: 10.1016/j.compstruct.2018.05
Yeh, M.K. and Hsieh, T.H. (2008), "Dynamic properties of sandwich beams with MWNT/polymer nanocomposites as core materials", *Compos. Sci. Technol.*, **68**(14), 2930-2936.
Yeh, M.K., Tai, N.H. and Liu, J.H. (2009), "Mechanical behavior of phenolic-based composites reinforced with multi-walled carbon nanotubes", *Carbon*, **44**(1), 1-9.
Zhou, X., Wang, K.W. and Bakis, C. (2004), "The investigation of carbon nanotube based polymers for improved structural damping", *Proceedings of SPIE on Smart Structures and Materials*, San Diego, CA, USA, April.
Zhu, P., Lei, Z.X. and Liew, K.M. (2012), "Static and free vibration analyses of carbon nanotube-reinforced composite plates using finite element method with first order shear deformation plate theory", *Compos. Struct.*, **94**(4), 1450-1460.

CC